

**Raman Spectroscopic Study of High Temperature  
Rare Earth Metal - Rare Earth Halide Solutions:  
Ln-LnX<sub>3</sub>- and LnX<sub>2</sub>-LnX<sub>3</sub>-(LiX-KX)<sub>eu</sub> Systems  
(Ln: Nd, Ce; X: Cl, I)**

**Zur Erlangung des akademischen Grades eines  
DOKTORS DER NATURWISSENSCHAFTEN  
(Dr. rer. nat.)  
von der Fakultät für Chemie und Biowissenschaften  
der  
Universität Karlsruhe (TH)  
angenommene**

**DISSERTATION**

**von  
M. Sc. Verónica María Rodríguez Betancourt  
aus Guadalajara, Jal., Mexiko**

**Dekan: Prof. Dr. M. Metzler**

**1. Gutachter: Priv. Doz. Dr. D. Nattland**

**2. Gutachter: Prof. Dr. M. Kappes**

**Tag der mündlichen Prüfung: 17.07.03**

# Index

<b>Abstract.</b> . . . . .	<b>1</b>
<b>Zusammenfassung.</b> . . . . .	<b>3</b>
<b>1. Introduction.</b> . . . . .	<b>4</b>
<b>2. Basic Concepts of Raman Spectroscopy.</b> . . . . .	<b>9</b>
2.1. Classical Description of Raman Spectroscopy. . . . .	9
2.2. Origin of the Raman Spectrum. . . . .	10
2.3. Depolarization ratios of Raman Bands . . . . .	12
2.4. Normal Modes of Vibration of the Molecules. . . . .	13
2.5. Symmetry and Selection Rules. . . . .	15
2.6. Presentation of a Spectrum. . . . .	17
2.7. Fluorescence. . . . .	18
2.8. Blackbody Radiation. . . . .	19
<b>3. Experimental Section.</b> . . . . .	<b>21</b>
3.1. Preparation of Chemicals: Ln Metals, LnCl <sub>3</sub> , LnI <sub>x</sub> , Alkali Halides (LiX and KX) and LnX <sub>2</sub> -LnX <sub>3</sub> -(LiX-KX) <sub>eu</sub> Mixtures. . . . .	22
3.2. Construction of the Optical Cells. . . . .	25
3.2.1. Cell 1: Quartz Cell. . . . .	25
3.2.2. Cell 2: Windowless Cell with Internal Furnace. . . . .	27
3.2.3. Cell 3: Windowless Cell with External Furnace. . . . .	27
3.3. Description of the Raman Spectrometer. . . . .	29
3.4. Experimental Procedures. . . . .	30

3.4.1. Preparation of the Sample: Quartz Cell and Windowless Cells. . . . .	30
3.4.2. Recording of the Raman Spectra. . . . .	31
<b>4. Experimental Problems, Spectra Analysis and Error Discussion. . . . .</b>	<b>33</b>
4.1. Experimental Problems. . . . .	33
4.1.1. Cell Corrosion. . . . .	33
4.1.2. Background Emission of Thermal Radiation. . . . .	34
4.1.3. Fluorescence. . . . .	36
4.1.4. Metal Dissolution in Rare Earth Halide-Alkali Halide Mixtures. . . . .	38
4.1.5. Film Formation. . . . .	38
4.2. Data Analysis and Error Discussion. . . . .	39
4.2.1. Analysis of the Experimental Data. . . . .	40
4.2.2. Error Discussion (Intensities, Wavenumber, Temperature, Concentration). . . . .	42
<b>5. Raman Spectra Ln-LnCl<sub>3</sub> (Ln = Nd, Ce) Melts. . . . .</b>	<b>43</b>
5.1 Nd-NdCl <sub>3</sub> Melts. . . . .	44
5.1.1. NdCl <sub>3</sub> . . . . .	44
5.1.2. NdCl <sub>2</sub> . . . . .	47
5.1.3. (NdCl <sub>3</sub> ) <sub>x</sub> -(LiCl-KCl) <sub>eu, 1-x</sub> . . . . .	49
5.1.4. (NdCl <sub>2</sub> ) <sub>x</sub> -(LiCl-KCl) <sub>eu, 1-x</sub> . . . . .	53
5.1.5. (NdCl <sub>3</sub> ) <sub>x</sub> -(NdCl <sub>2</sub> ) <sub>y</sub> -(LiCl-KCl) <sub>eu, 1-x-y</sub> . . . . .	54
5.2. Ce-CeCl <sub>3</sub> Melts. . . . .	56
5.2.1. CeCl <sub>3</sub> and (CeCl <sub>3</sub> ) <sub>x</sub> -(LiCl-KCl) <sub>eu, 1-x</sub> . . . . .	56
5.2.2. (Ce) <sub>y</sub> -(LiCl-KCl) <sub>eu, 1-y</sub> . . . . .	59
5.2.3. (CeCl <sub>3</sub> ) <sub>x</sub> -(Ce) <sub>y</sub> -(LiCl-KCl) <sub>eu, 1-x-y</sub> . . . . .	61
<b>6. Raman Spectra of Ln-LnI<sub>3</sub> (Ln = Ce, Nd) Melts . . . . .</b>	<b>67</b>
6.1. Ce- CeI <sub>3</sub> Melts. . . . .	67
6.1.1. CeI <sub>3</sub> . . . . .	67

6.1.2. $\text{CeI}_2$ .	72
6.1.3. $(\text{CeI}_3)_x-(\text{CeI}_2)_y$ .	73
6.1.4. $(\text{CeI}_3)_x-(\text{LiI-KI})_{\text{eu}, 1-x}$ .	75
6.1.5. $(\text{CeI}_2)_y-(\text{LiI-KI})_{\text{eu}, 1-y}$ .	76
6.1.6 $(\text{CeI}_3)_x-(\text{CeI}_2)_y-(\text{LiI-KI})_{\text{eu}, 1-x-y}$ .	77
6.2. Nd-NdI <sub>3</sub> Melts.	79
6.2.1. NdI <sub>3</sub> .	79
6.2.2. NdI <sub>2</sub> .	79
6.2.3. $(\text{NdI}_3)_x-(\text{NdI}_2)_{1-x}$ .	80
6.2.4. $(\text{NdI}_3)_x-(\text{LiI-KI})_{\text{eu}, 1-x}$ .	81
6.2.5 $(\text{NdI}_3)_x-(\text{NdI}_2)_y-(\text{LiI-KI})_{\text{eu}, 1-x-y}$ .	83
<b>7. Discussion.</b>	<b>85</b>
7.1. Structural and Physicochemical Data of Solid and Liquid LnX <sub>3</sub> and LnX <sub>2</sub> .	85
7.2. LnX <sub>3</sub> and LnX <sub>3</sub> -(LiX-KX) <sub>eu</sub> Melts.	88
7.2.1. LnX <sub>3</sub> .	88
7.2.2. LnX <sub>3</sub> -(LiX-KX) <sub>eu</sub> .	94
7.3. LnX <sub>2</sub> and LnX <sub>2</sub> -(LiX-KX) <sub>eu</sub> Melts.	97
7.3.1. NdCl <sub>2</sub> .	97
7.3.2. CeI <sub>2</sub> and NdI <sub>2</sub> .	100
7.3.3. LnCl <sub>2</sub> -(LiCl-KCl) <sub>eu</sub> .	102
7.3.4. LnI <sub>2</sub> -(LiI-KI) <sub>eu</sub> .	103
7.4. Mixed Rare Earth Metal-Rare Earth Halide (Ln-LnX <sub>3</sub> ) Systems.	104
7.4.1. Alkali Metal-Alkali Halide Solutions: F centers, Bipolaron and Drude Electron.	104
7.4.2. Mixed Valence States in Molten Salts: Two Site Small Polaron Model.	105
7.4.3. $(\text{NdCl}_3)-(\text{NdCl}_2)-(\text{LiCl-KCl})_{\text{eu}}$ .	106
7.4.4. $(\text{CeCl}_3)-(\text{Ce})-(\text{LiCl-KCl})_{\text{eu}}$ .	108
7.4.5. $(\text{CeI}_3)-(\text{CeI}_2)-(\text{LiI-KI})_{\text{eu}}$ .	109

<b>Appendix.</b> . . . . .	<b>111</b>
A1. Phase Diagrams and Literature Data of Selected Compounds. . . . .	111
A2. Raman Spectra of the Alkali Halide Eutectic Mixtures. . . . .	116
A3. Raman Spectra of $(\text{NdCl}_3)_x$ - $(\text{NdCl}_2)_y$ - $(\text{LiCl-KCl})_{\text{eu}, 1-x-y}$ Melts. . . . .	117
A4. Raman Spectra of $(\text{CeCl}_3)_x$ - $(\text{Ce})_y$ - $(\text{LiCl-KCl})_{\text{eu}, 1-x-y}$ Melts. . . . .	122
A5. Raman Spectra of $(\text{CeI}_3)_x$ - $(\text{CeI}_2)_y$ - $(\text{LiI-KI})_{\text{eu}, 1-x-y}$ Melts. . . . .	125
A6. Raman Spectra of $(\text{NdI}_3)_x$ - $(\text{NdI}_2)_y$ - $(\text{LiI-KI})_{\text{eu}, 1-x-y}$ Melts. . . . .	132
<b>Manufacturer List.</b> . . . . .	<b>136</b>
<b>References.</b> . . . . .	<b>137</b>

## Abstract

In this work new Raman spectroscopic experiments on rare earth metal-rare earth trihalide melts ( $\text{Ln-LnX}_3$  and  $\text{LnX}_2\text{-LnX}_3$ ;  $\text{Ln}=\text{Ce, Nd}$ ;  $\text{X}=\text{Cl, I}$ ) and their mixtures in alkali halide eutectic solvents ( $(\text{LiX-KX})_{\text{eu}}$ ;  $\text{X}=\text{Cl, I}$ ) are presented. The neodymium and cerium systems have been selected because their metal-metal trihalide melts exhibit very different behavior of the specific electric conductivity as function of the metal concentration. On the one hand, in the Ce-systems it increases strongly which may be due to the formation of mobile electronic defect states. On the other hand, in the Nd-systems it shows only a shallow maximum at the composition of  $\text{NdX}_{2.5}$ . For this behavior an intervalence charge transfer mechanisms was suggested. In this context an important objective is to study a possible influence of the specific types of electronic defect states in these systems on the microscopic structure. The main experimental challenge was the strong corrodibility of these melts. To overcome this difficulty a new windowless Raman cell had to be developed. In such a set up the exciting laser beam was focused through a protecting optical window onto the sample contained in a corrosion resistant crucible (e. g. glassy carbon). The Raman spectrum was measured in the back scattering geometry. The optical window had no direct contact with the high temperature melt. The limitations are given by a possible contamination of the window by sublimated traces of the sample.

The main results can be summarized as follows:

- The Raman spectra of following trihalide systems have been measured for the first time:  $\text{CeCl}_3$ ,  $\text{CeI}_3$ ,  $\text{NdI}_3$  and their mixtures in the respective alkali halide eutectic solvent. The structure of the  $\text{LnX}_3$  in the solvent can be characterized by octahedral complexes. The force constants decrease from the chlorides to the iodides.
- The Raman spectra of the following dihalides have been observed in this work:  $\text{NdCl}_2$ ,  $\text{CeI}_2$  and their mixtures in the alkali halide solvent. Interestingly,  $\text{CeCl}_2$  might form as

intermediate species on doping  $\text{CeCl}_3$  with Ce. It is not a stable compound in the Ce- $\text{CeCl}_3$  phase diagram.

- With respect to the above mentioned main objective the following conclusions can be drawn:

- (i) On mixing of  $\text{NdCl}_2$  with  $\text{NdCl}_3$  in  $(\text{LiCl-KCl})_{\text{eu}}$  the undisturbed spectra of both components can be observed simultaneously. This is in agreement with the suggested intervalence charge transfer hopping mechanism if one assumes a hopping rate below  $10^{12}$ .
- (ii) Even though  $\text{CeCl}_2$  might form as intermediate, in the equilibrium spectra of liquid Ce- $\text{CeCl}_3$ - $(\text{LiCl-KCl})_{\text{eu}}$  only the typical  $\text{CeCl}_6^{3-}$ -octahedra can be identified. This supports the assumption that in these systems the electronic defect states are probably mobile Drude-like electrons which do not lead to new Raman detectable species. A qualitatively similar observation was made for  $\text{CeI}_2$ - $\text{CeI}_3$ - $(\text{LiI-KI})_{\text{eu}}$  melts.

## Zusammenfassung

In der vorliegenden Arbeit werden neue spektroskopische Ramanexperimente an Seltenerdmetall- Seltenerdmetalltrihalogenid Schmelzen ( $\text{Ln-LnX}_3$  und  $\text{LnX}_2\text{-LnX}_3$ ;  $\text{Ln}=\text{Ce, Nd}$ ;  $\text{X}=\text{Cl, I}$ ) und deren Mischungen mit flüssigen eutektischen Alkali-Halogeniden  $[(\text{LiX-KX})_{\text{eu}}; \text{X}=\text{Cl, I}]$  dargestellt. Die Neodym- und Cer-Systeme wurden ausgewählt weil ihre Metall-Metalltrihalogenid-Schmelzen sehr unterschiedliches Verhalten der spezifischen elektrischen Leitfähigkeit mit der Metallkonzentration zeigen. Einerseits steigt sie in den Cer-Systemen sehr stark an, was mit der Bildung von beweglichen elektronischen Defektzuständen erklärt werden kann. Andererseits, verläuft sie bei den Nd-Systemen nur durch ein flaches Maximum bei einer Zusammensetzung von  $\text{NdX}_{2.5}$ . Für dieses Verhalten wurde ein *Intervalence Charge Transfer* Mechanismus vorgeschlagen. Eine wichtige Zielsetzung ist in diesem Zusammenhang, einen möglichen Einfluss der spezifischen Art des elektronischen Defektzustandes in diesen Systemen auf die mikroskopische Struktur zu untersuchen. Die wesentliche experimentelle Herausforderung war die starke Korrosivität dieser Schmelzen. Um diese Schwierigkeiten zu überwinden, musste eine neue fensterlose Ramanzelle entwickelt werden. In diesem Aufbau wurde der anregende Laserstrahl durch das die Probe schützende optische Fenster auf die Probe fokussiert, die sich in einem korrosionsresistenten Tiegel befand (z. B. aus glasartigen Kohlenstoff). Das Ramanspektrum wurde in Rückstreuengeometrie gemessen. Das optische Fenster hatte keinen direkten Kontakt mit der Hochtemperaturschmelze. Diese experimentelle Vorgehensweise hat ihre Grenzen in der möglichen Kontamination des Fensters durch sublimierten Rest der Probe.

Die wesentlichen Ergebnisse können wie folgt zusammengefasst werden:

- Die Raman Spektren der folgenden Trihalogenid Systeme wurden zum ersten Mal gemessen:  $\text{CeCl}_3$ ,  $\text{CeI}_3$ ,  $\text{NdI}_3$  und ihre Mischungen im jeweiligen eutektischen Alkalihalogenidlösungsmittel. Die Struktur des  $\text{LnX}_3$  im Lösungsmittel kann durch



oktaedrische Komplexe gekennzeichnet werden. Die Kraft konstante nimmt von den Chlorverbindungen zu den Jodiden ab.

- Die Raman Spektren der folgenden Dihalogenide wurden in dieser Arbeit beobachtet:  $\text{NdCl}_2$ ,  $\text{CeI}_2$  und ihre Mischungen im eutektischen Alkalihalogenidlösungsmittel. Interessanterweise bildet sich  $\text{CeCl}_2$  möglicherweise als intermediäre Spezies, wenn  $\text{CeCl}_3$  mit Cer-Metall dotiert wird. Im  $\text{Ce-CeCl}_3$  Phasendiagramm ist es nicht als stabile Verbindung erkannt.
- In Bezug auf die oben erwähnt Hauptzielsetzung können folgende Schlussfolgerungen gezogen werden:
  - (i) Beim Mischen von  $\text{NdCl}_2$  mit  $\text{NdCl}_3$  in  $(\text{LiCl-KCl})_{\text{eu}}$  können die ungestörten Spektren der beiden Bestandteile nebeneinander beobachtet werden. Dies ist in Übereinstimmung mit dem vorgeschlagenen *Intervalence Charge Transfer* Mechanismus, wenn man eine Platzwechselfrequenz des Elektrons von weniger als  $10^{12}$  Hz zugrunde legt.
  - (ii) Obwohl sich  $\text{CeCl}_2$  als Intermediär bildet, können in den Gleichgewichtsspektren von flüssigem  $\text{Ce-CeCl}_3-(\text{LiCl-KCl})_{\text{eu}}$  lediglich die typischen  $\text{CeCl}_6^{3-}$ -Oktaeder identifiziert werden. Dieses stützt die Annahme, dass in diesen Systemen die elektronischen Defektzustände vermutlich bewegliche Drude Elektronen sind, die nicht zu neuen Spezies führen, die im Ramanspektrum nachweisbar sind. Eine qualitativ ähnliche Beobachtung wurde für  $\text{CeI}_2\text{-CeI}_3\text{-(LiI-KI)}_{\text{eu}}$  Schmelzen gemacht.

## 1. Introduction

The aim of this investigation is the study of the microscopic structure of rare earth halide systems in the molten state applying Raman spectroscopy. More specifically, we are interested in a possible influence on the microscopic structure as molten rare earth trihalide systems are doped with the respective rare earth metal or with its subhalide.

In general, metal molten salt solutions may be subdivided in two main prototypical groups with respect to different mechanisms for electron localization. First, the alkali metal-alkali halide systems show over a miscibility gap a homogeneous phase range where the system undergoes a continuous transition from a liquid ionic conductor (the pure liquid salt) to a metallic system (the pure liquid metal). No stable subhalide can be found. Instead, in the salt rich range the electronic defect states are localized F-center like states and spin paired (bipolaronic) states in equilibrium with mobile nearly-free Drude electrons. The first can be identified by their characteristic absorption band whereas the latter lead to a strong increase of the specific electronic conductivity with increasing metal concentration. The alkali metal-alkali halide systems exhibit a non metal-to-metal transition in the concentration range of the metal of  $x_{\text{NMM}} \approx 0.2$ . The systems have been studied quite extensively and are described in some reviews (Bredig 1964, Warren 1985, Nattland 1996, Freyland 1994, Freyland 1995).

The second group of metal-molten salt systems is represented by mixed valence transition metal-transition metal halide systems like tantalum or niobium halides. Doping of pentavalent metal halide containing melts with the respective transition metal lead to subhalide species like Ta(IV)-chloride. Here, electron transport takes place by hopping from

one Ta-site to another. This intervalence charge transfer leads to a maximum of electronic conductivity at a concentration ratio of  $\text{Ta(V)}/\text{Ta(IV)} \approx 1$ . The value of the electronic conductivity does exceed considerably that of the ions (Stöhr 1999, Stöhr 1999a).

In this respect the rare earth metals and their trihalides are of particular interest. As can be seen for the Ln-LnCl<sub>3</sub> system in Fig 1.1 and for Ln-LnI<sub>3</sub> system in Fig 1.2 they display both limiting cases described above. As the lighter rare earth metal (La and Ce) are dissolved in their molten trihalides the conductivity rises almost as steep as in the alkali metal-alkali halide systems. Thus, the mobile electronic species must exist in these systems. On the other hand, the neodymium systems show a shallow maximum of the conductivity. In these systems stable subhalides exist. This resembles the intervalence charge transfer transport mechanism. For Nd-NdCl<sub>3</sub> (Terakado 2002a) and for Nd-NdI<sub>3</sub> (Zein El Abedin 2002) this was suggested recently on account of optical absorption and conductivity measurements.

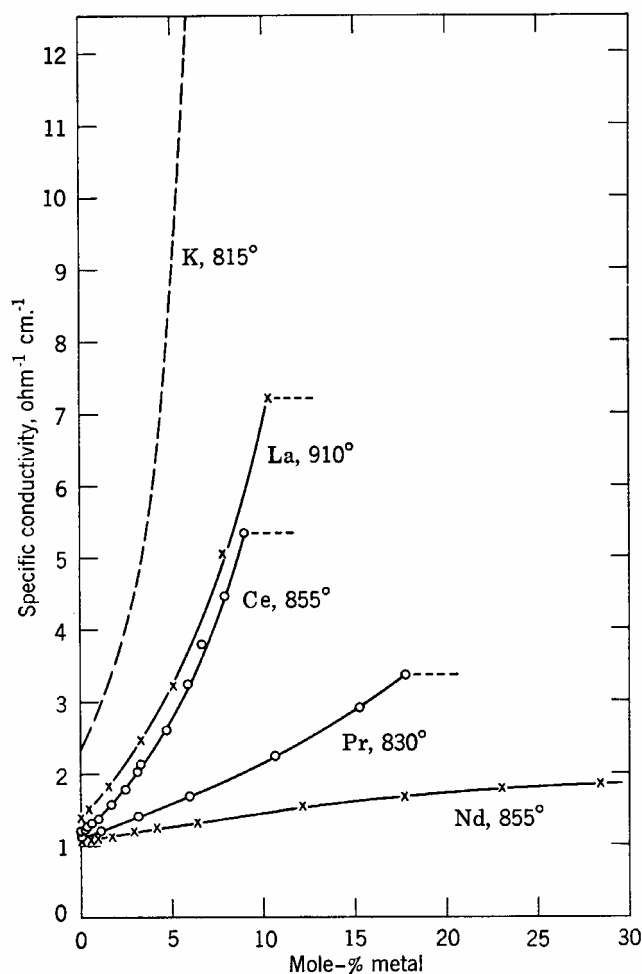


Figure 1.1: Specific conductivity in rare earth metal-rare earth metal chloride systems (Bredig 1964).

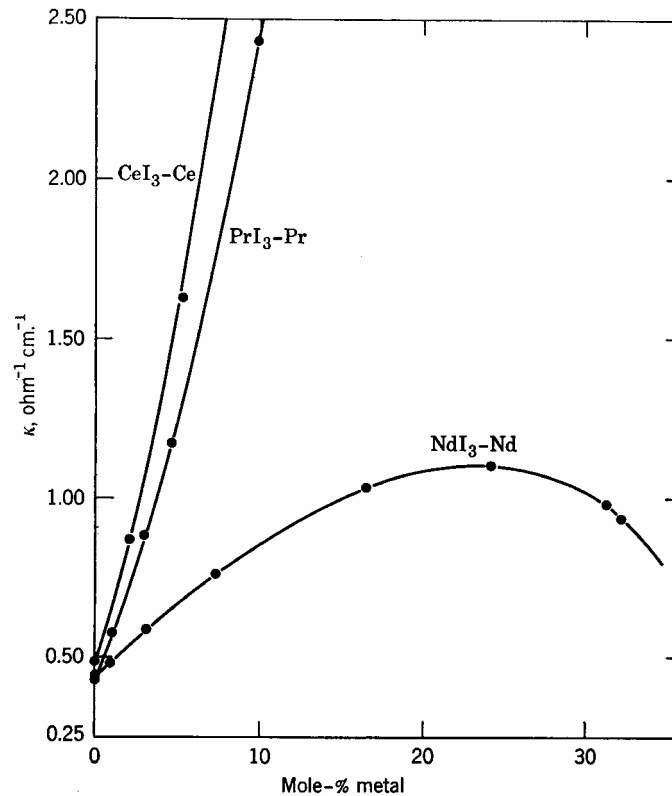


Figure 1.2: Specific conductivity in rare earth metal-rare earth metal iodide systems (Bredig 1964).

Besides the electronic properties, the modifications of the microscopic structure of liquid  $\text{LnX}_3$  systems as they are doped with Ln metal are of special interest. In this respect, Raman spectroscopy can provide valuable new information on a possible interplay between electronic and microscopic structure: does the structure of the Raman active species in the melt change on doping? Do new species appear as the liquid trihalide is mixed with the respective metal or with the dihalide?

The microscopic structures of rare earth trihalides and their molten mixtures with alkali halides (AX) have been extensively studied by G. M. Papatheodorou's research group at the University of Patras by means of vibrational Raman spectroscopy (Papatheodorou 1975, Papatheodorou 2002, Photiadis 1994, Photiadis 1998, Børresen 1996, Dracopoulos 1998). They found that in the solid state the microscopic structure of pure  $\text{LnCl}_3$  change along the lanthanide series, depending on the size of the metal atom. Thus, for large  $\text{Ln}^{3+}$  cations the trihalides are hexagonal, with a nine-fold coordination of Ln. For small  $\text{Ln}^{3+}$  cations the structures are monoclinic or rhombohedral, being the Ln six-fold coordinated. For certain

intermediate cations the trihalides are orthorhombic with an eight-fold coordination. In the liquid state on the other hand, the Raman patterns indicate a nearly common structure consisting of a loose network of edge bridged distorted octahedral (Ln with six-fold coordination). Furthermore, in rich alkali halide molten mixtures ( $x_{NaCl_3} \leq 0.25$ ) the normal octahedral species  $LnX_6^{3-}$  dominate (Pavlatou 1997, Photiadis 1993, Photiadis 1998).

Contrary to the  $LnX_3$ , the  $Ln-LnX_3$  systems and their mixtures with alkali halide mixtures had not been investigated up to now by Raman spectroscopy. Probably this is mainly due to their chemical corrosive properties and in the case of  $LnX_2$  to the problems of disproportionation at high temperatures, i.e.  $3LnX_2 \rightarrow 2LnX_3 + Ln$  (Gmelin 1982, Lavtep 1986).

To overcome at least parts of these difficulties a new approach is presented in this work. On the one hand, we use a Raman spectrometer with a CCD camera for fast experiments. A microscope objective with a short working distance allows a highly focused laser beam and small sample sizes. On the other hand we employ windowless cells to avoid cell corrosion by the melt. These cells including furnace have to be specially designed for the optical set up.